High Pressure Induces Scrapie-like Prion Protein Misfolding and Amyloid Fibril Formation†

Joan Torrent,‡ Maria Teresa Alvarez-Martinez,§ Marie-Cécile Harricane,|| Frédéric Heitz,|| Jean-Pierre Liautard,§ Claude Balny,‡ and Reinhard Lange*,‡

Université de Montpellier 2, EA3763, Place Eugène Bataillon, F-34095 Montpellier cédex 5, France, INSERM U431, IFR 122, Place Eugène Bataillon, F-34095 Montpellier cédex 5, France, and CRBM, CNRS-FRE 2593, IFR 122, 1919 Route de Mende, F-34293 Montpellier cédex 5, France

Received January 8, 2004; Revised Manuscript Received March 24, 2004

ABSTRACT: Our understanding of conformational conversion of proteins in diseases is essential for any diagnostic and therapeutic approach. Although not fully understood, misfolding of the prion protein (PrP) is implicated in the pathogenesis of prion diseases. Despite several efforts to produce the pathologically misfolded conformation in vitro from a recombinant PrP, no positive result has yet been obtained. Within the "protein-only hypothesis", the reason for this hindrance may be that the experimental conditions used did not allow selection of the pathway adopted in vivo resulting in conversion into the infectious form. Here, using a pressure perturbation approach, we show that recombinant PrP is converted to a novel misfolded conformer, which is prone to aggregate and ultimately form amyloid fibrils. A short incubation at high pressure (600 MPa) of the truncated form of hamster prion protein ($SHaPrP_{90-231}$) resulted in the formation of pre-amyloid structures. The mostly globular aggregates were characterized by ThT and ANS binding, and by a β-sheet-rich secondary structure. After overnight incubation at 600 MPa, amyloid fibrils were formed. In contrast to pre-amyloid structures, they showed birefringency of polarized light after Congo red staining and a strongly decreased ANS binding capacity, but enhanced ThT binding. Both aggregate types were resistant to digestion by PK, and can be considered as potential scrapie-like forms or precursors. These results may be useful for the search for compounds preventing pathogenic PrP misfolding and aggregation.

The devastating symptoms of transmissible spongiform encephalopathies (TSEs) or prion diseases, for which no cure is available, are caused by an aberrant conformational change of a protein (i.e., the cellular prion protein) leading to its deposition in the form of amyloid fibrils (*1*). Similar events occur in other neurodegenerative (conformational) diseases (*2*), such as Alzheimer's disease, Parkinson's disease, and Huntington syndrome, which have become a major concern for public health as life expectancy increases. The specificity of prion diseases is that they are transmissible, not only naturally but also under experimental conditions. Their transmissibility is explained by the "protein-only" hypothesis, stating that prions are infectious agents capable of inducing their own replication (*3*). Although this hypothesis has not yet been proven, considerable experimental data argue that prions are composed exclusively of an abnormal pathological conformer (PrP^{Sc})[1] of a host-encoded cellular prion protein (PrP^{C}) that is widely expressed in neurons and glia in the central nervous system (*4*, *5*).

However, two central problems remain to be resolved. The first one concerns the structure of PrP^{Sc}. The second one concerns the mechanism by which PrP^{C} converts to PrP^{Sc}. Several properties of the pathological form are known: whereas PrP^{C} is rich in α-helical structure, monomeric, and susceptible to enzyme digestion, PrP^{Sc} has a large content of β-sheet, forms amyloid fibrils, and is strongly resistant to proteolytic digestion (*6*). Accordingly, many attempts have been undertaken to destabilize the native PrP^{C} structure and form amyloid structures. These include the use of high temperature, chemical denaturants, salts, and extreme pH conditions (*7*). Although the possibility of experimentally producing a disease-causing protein would finally prove the protein-only hypothesis, and would also provide a structural model useful for the identification of potential therapeutic agents, attempts to convert recombinant PrP to a scrapie-like form in vitro have never resulted in an infectious structure. To explain this failure, we hypothesized that acquisition of the disease-causing conformation depends on folding pathways which are difficult to achieve, and that the experimental conditions used so far did not enable conversion to such a structure.

† Supported by GIS − prions (Ministery of Research), ATC − prions (INSERM), and Human Science Frontier Program (HSFP).

* To whom correspondence should be addressed: Reinhard Lange, EA3763, CC 105, Université de Montpellier 2, Place Eugène Bataillon, F-34095 Montpellier cédex 5, France. Tel: +33.467.14.33.85. E-mail: lange@montp.inserm.fr.

‡ Université de Montpellier 2.

§ INSERM U431, IFR 122.

|| CRBM, CNRS-FRE 2593.

[1] Abbreviations: ANS, 8-anilino-1-naphthalene sulfonate; ThT, thioflavin T; PrP, prion protein; PrP^{C}, cellular isoform; PrP^{Sc}, pathogenic isoform; $SHaPrP_{90-231}$, Syrian hamster recombinant PrP consisting of residues 90−231; PK, proteinase K; FTIR, Fourier transform infrared.

10.1021/bi049939d CCC: $27.50
Published on Web 05/13/2004

Our approach to find a way to convert PrP^C to PrP^{Sc} is the use of high pressure combined with several types of spectroscopy. Indeed, pressure is known to induce structural changes in proteins, which are different from those induced by other denaturing agents. Therefore, this much less used thermodynamic parameter provides an elegant alternative to investigate new aspects of protein misfolding and refolding to alternative conformations, and is promising to study structural changes of PrP. Pressure frequently promotes the generation of unfolded protein states retaining significant residual secondary structure, and stabilizes unfolding intermediate states (*8*). Therefore, pressure is used increasingly to study conformational stability and aggregation of proteins, such as those implicated in amyloidogenic diseases (*9*, *10*).

Recently, we applied this method to study structural changes of the $SHaPrP_{90-231}$ (*11*, *12*). At low protein concentration (0.5−0.8 mg/mL), the application of pressure (up to 600 MPa) revealed hitherto unknown misfolding routes. In addition, pressure was used to convert temperature-induced PrP aggregates from an irreversible to a reversible tertiary and secondary structural change. Here we extend this work to higher protein concentration (2−5 mg/mL). We provide a first demonstration that high-pressure induces PrP misfolding and leads to the formation of amyloid fibrils.

METHODS

Prion Protein. Recombinant $SHaPrP_{90-231}$ was prepared from *Escherichia coli* BL21(DE3) as described (*12*). The sequence of this protein corresponds to the sequence of the PK-resistant core of PrP^{Sc}, denoted PrP 27−30, which transmits the disease.

Structural Characterization under Pressure. For high-pressure experiments, the protein was dissolved in 20 mM Tris-HCl buffer at pH 8.5. This buffer was selected for its relatively low-pressure pH dependency on pressure (*13*). The final protein concentration was 2 mg/mL, if not specified otherwise. Following each pressure change, typically in steps of 30 MPa, the sample was allowed to equilibrate for 5 min before the next measurement. Experiments were performed at 40 °C.

Fluorescence Spectroscopy and Light Scattering Measurements. Fluorescence emission spectra were recorded with an Aminco-Bowmann Series 2 luminescence spectrometer (SLM Aminco), modified to accommodate a thermostated pressure cell. Tyr and Trp fluorescence was measured by exciting at 265 nm (4-nm slit). The emission slit was 4 nm. ANS and ThT were used as probes to measure extrinsic fluorescence. For ANS binding studies, fluorescence was excited (4-nm slit) at 360 nm, and emission spectra (8-nm slit) were collected (accumulation of three scans). The ANS concentration was 50 μM. For ThT, assays were performed with a ThT concentration of 10 μM. Fluorescence emission spectra (average of three scans) were obtained with an excitation wavelength of 442 nm and excitation and emission slits of 4 and 8 nm, respectively. Small contributions due to scattered light were subtracted from the signal as follows: a protein sample spectrum in the absence of the corresponding fluorescent probe was collected at each pressure so that contributions from light scattering could be subtracted. Protein aggregation was followed by monitoring the changes in light scattering intensity at 340 nm (4-nm slit widths).

Structural Characterization at Atmospheric Pressure. Overnight incubation at 600 MPa led to assembly processes between the aggregates, and their subsequent deposition from solution. Following decompression and before performing analyses, the recovered aggregates were disrupted through the shearing and cavitation forces produced by ultrasound (sonication). Analyses were performed using the entire protein sample, without pelleting the aggregate, unless stated otherwise.

ThT and ANS Binding. Aliquots of soluble and aggregated PrP (2 mg/mL) were diluted 40 times with 50 mM Tris-HCl, pH 8.5, and incubated with either 10 μM ThT for 1 min or 50 μM ANS for 10 min at room temperature before monitoring fluorescence. Fluorescence measurements were performed at 21 °C with a FluoroMax-2 fluorimeter (Jobin Yvon-Spex) with a 1-cm rectangular cuvette. For ANS spectra, excitation was at 385 nm (2-nm slit). Each emission spectrum (2-nm slit) was the average of three scans. ThT emission spectra were recorded after excitation at 450 nm (excitation slit was 4 nm; emission slit was 4 nm), with each spectrum being the average of three scans. Contributions due to scattered light were subtracted from the signal as indicated above.

FTIR Spectroscopy. Spectra (500 scans accumulation) were recorded at ambient conditions using an IFS28 spectrometer equipped with a DTGS detector (Bruker) at a spectral resolution of 2 cm^{-1} and analyzed by OPUS/IR2 program. For comparison of soluble and aggregated protein, all spectra were recorded with dry samples. Comparison of dried protein and samples in solution did not reveal significant changes in their FTIR spectra (*14*, *15*). Samples, after pelleting the aggregate (8500*g* for 2 min) and resuspending in buffer, were prepared by deposition onto a fluorine plate, where the solvent was allowed to evaporate overnight at room temperature. Secondary structure prediction was based on a combination of Fourier self-deconvolution with a band-fitting procedure (*16*, *17*). Fourier self-deconvolution, a mathematical technique of band-narrowing, was performed after baseline correction. A half bandwidth of 19 cm^{-1} and an enhancement factor (K) of 1.6 were used (*18*). For the band-fitting, initial band frequencies were determined from the second derivatives of the deconvoluted spectra.

Congo Red Staining and Birefringence. An aggregated protein suspension was air-dried on a glass microscope slide. The sample was stained and examined as described (*12*).

PK Resistance. Protease resistance was assayed by incubating sample aliquots (soluble or aggregated PrP), in 20 mM Tris-HCl pH 8.5 containing various concentrations of PK for 1 h at 37 °C. PrP-PK protein concentration ratios (w:w) were from 166:1 to 3:1. Digestion reactions were terminated by addition of Pefabloc (Roche Diagnostics GmbH) to a final concentration of 3 mM. Finally, digestion of samples was assessed by SDS−PAGE.

Transmission Electron Microscopy (TEM). The aggregates obtained by pressurization were diluted to a protein concentration of 0.2 mg/mL, deposited onto formwar-carbon-coated grids and negatively stained with 2% aqueous uranyl acetate. Grids were examined using a JEOL $1200EX^2$ electron microscope at an accelerating voltage of 80 KV.

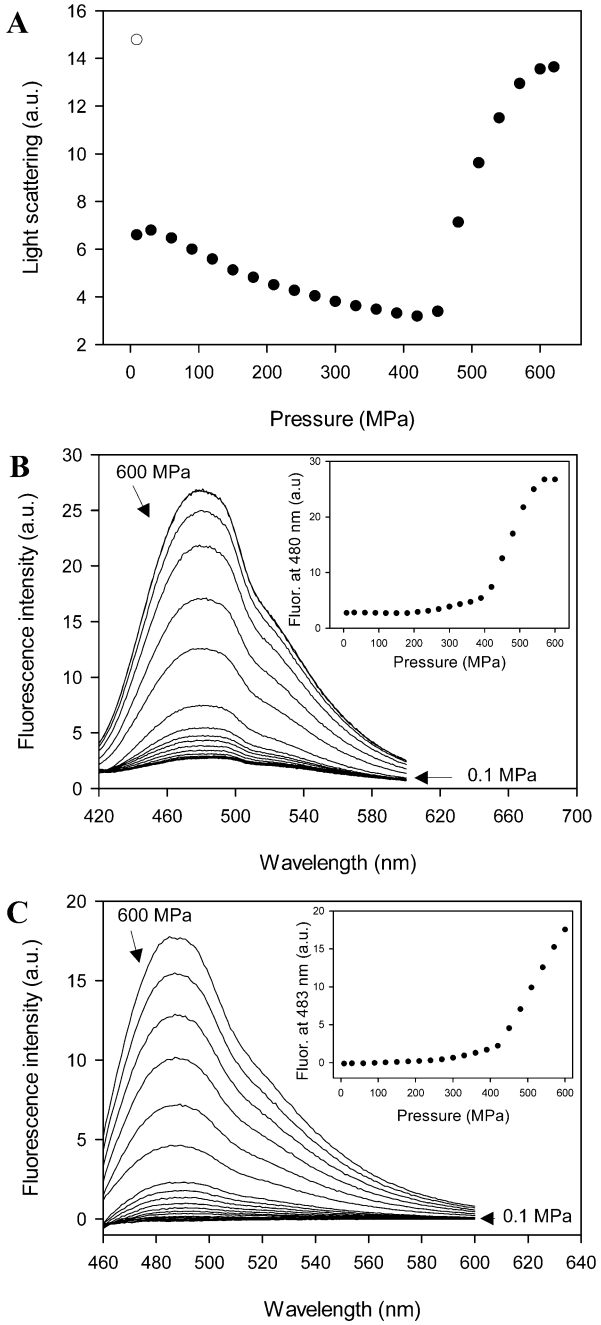

FIGURE 1: (A) Pressure-induced aggregation of PrP as measured by light scattering at 340 nm (●). Light scattering measured after pressure release (○). In situ ANS (B) and ThT (C) binding to PrP upon increasing pressure, monitored by changes in fluorescence intensity. The insets show the change in fluorescence intensity at 480 nm (ANS) and 483 nm (ThT) at increasing pressures. a.u., arbitrary units.

RESULTS

PrP Aggregation under High Pressure. As evidenced by the sharp increase of light scattering intensity, PrP (2 mg/mL) aggregates at pressures greater than 450 MPa (Figure 1A). This aggregation process is irreversible and is paralleled by the in situ protein capacity to bind ANS and ThT, two extrinsic fluorescent probes (Figure 1B,C). For both ANS and ThT experiments, fluorescence emission spectra were only slightly distorted by light scattering, and after removal of this contribution, it became evident that the fluorescent profiles closely matched the pressure-dependent light scattering profile. Therefore, the increased ANS and ThT fluorescence obtained upon compression is a characteristic of the pressure-induced aggregates.

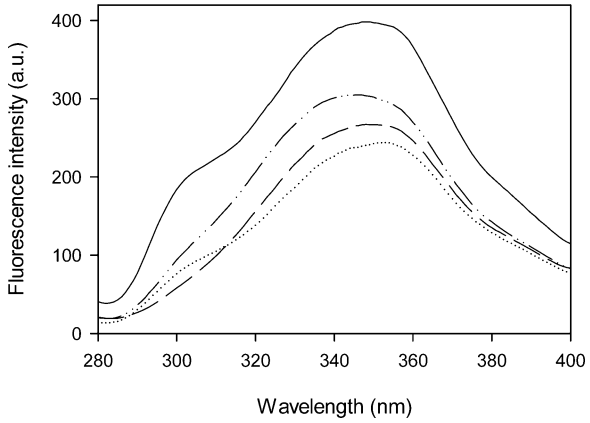

FIGURE 2: Fluorescence emission spectra of PrP upon excitation at 265 nm (exciting Tyr and Trp) as a function of pressure: atmospheric pressure (solid line), 450 MPa (dotted line), 600 MPa (dashed line), and atmospheric pressure after pressure release (dashed and dotted line).

Tertiary Structural Changes under High Pressure. Upon compression, the tertiary structural changes were monitored by intrinsic fluorescence spectroscopy (Figure 2). The fluorescence spectrum at atmospheric pressure showed two emission maxima, which correspond to tyrosines, at 307 nm, and to the two tryptophans, around 348 nm. At 450 MPa, i.e., in the absence of protein aggregation, the intensity of the fluorescence emission decreased, concomitantly with a 5-nm red shift of the maximum, suggesting that the Trp residues became even more water exposed. Upon further increase of pressure, i.e., during PrP aggregation, the fluorescence emission of Tyr progressively disappeared. This process was completely irreversible. No contribution of scattered light due to protein aggregation was apparent in the Tyr and tryptophan bands. Therefore, correction of intrinsic fluorescence emission spectra for light scattering was not necessary here.

Secondary Structural Changes after Transient Treatment at 600 MPa and Pressure Release. As shown in Figure 3A, the FTIR spectrum in the amide I region of native PrP is dominated by a strong band at 1656 cm^{-1}, reflecting a high proportion of α-helix and only little β-sheet structure, consistent with the NMR structure of the protein (*19*, *20*). The transient high-pressure treatment at 600 MPa (Figure 3B) resulted in profound spectral changes: the relative intensity of the 1656 cm^{-1} band decreased, and a new band appeared at 1621 cm^{-1}, reflecting a strongly decreased β-sheet structure. Concomitantly, the intensity at 1641 cm^{-1} increased, indicating an enhanced content of unordered structure. In Table 1, the IR bands are tentatively assigned to secondary structure elements (*16*, *17*). Within experimental errors, the secondary structure changed from 50% α-helix, 8% β-sheet, and 16% unordered structure in the native protein, to 31% α-helix, 22% β-sheet, and 31% unordered structure in the high-pressure treated protein.

Ultrastructure of PrP Aggregates Obtained after Transient Treatment at 600 MPa and Pressure Release. After pressure release, the nature of the PrP aggregates was characterized by Congo red staining and polarization microscopy. The bound dye did not exhibit blue-green birefringence, indicating

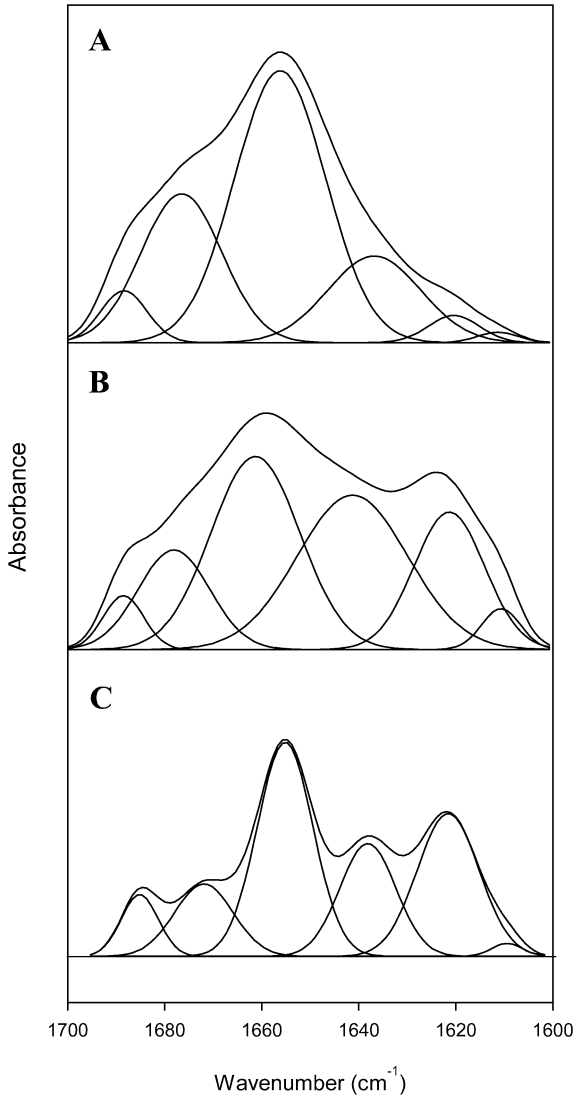

FIGURE 3: Fourier-deconvoluted and fitted IR spectra in the amide I region with individual Gaussian components of native PrP (A), pressure-induced aggregated form after transient treatment at 600 MPa (B), and aggregates obtained after overnight incubation at 600 Mpa (C).

that no amyloid structures were formed under this condition. The ultrastructure of the aggregates was assessed by TEM. Surveying the entire EM grid, distinct structural morphologies of PrP were observed: amorphous aggregates of spheroid structures (Figure 4A), and super-structures of these spheroids formed by linear association (Figure 4B). These results indicate that the aggregates formed after brief pressurization at 600 MPa, followed by decompression, are not yet organized in the form of amyloid fibrils. Rather, PrP adopts a partially unfolded conformation, with clustered hydrophobic regions exposed to the solvent, that are most likely involved in the formation of intermediates or byproducts of the assembly process into mature fibrillar structures. Thereafter we refer to them as "pre-amyloid structures".

PrP Structural Changes upon Prolonged Incubation at 600 MPa. Because formation of amyloid fibrils, as a result of incubating recombinant PrP at specific reaction conditions in the presence of guanidine hydrochloride, has been shown in previous studies to be a time-dependent process (*21*), we checked whether the incubation time had also an effect on the pressure-induced structural changes. During overnight

Table 1: IR Band Positions and Secondary Structure Assignments for the Amide I Band of Different Forms of $SHaPrP_{90-231}$

protein	band position (cm^{-1})	assignment	band area (%)
Native	1611	side-chains	1
	1621	β-sheet	3
	1637	unordered	16
	1656	α-helix	50
	1676	turns + loops	25
	1688	β-sheet	5
after transient treatment at 600 MPa	1611	side-chains	3
	1621	β-sheet	18
	1641	unordered	31
	1661	α-helix	31
	1678	turns + loops	13
	1688	β-sheet	4
after overnight incubation at 600 MPa	1610	side-chains	1
	1622	β-sheet	26
	1638	unordered	19
	1655	α-helix	35
	1672	turns + loops	12
	1685	β-sheet	7

pressurization at 600 MPa, assembly processes between aggregates were evidenced by protein deposition. The kinetics of deposition of the aggregated protein, followed by light scattering, was exponential and completed within 8 h. After pressure release, no light scattering was detected. Instead, a clear solution was observable by eye, and all protein was compacted on the bottom of the cuvette. The overnight incubation at 600 MPa had modified the properties of the pre-amyloid structures described above. Upon sonication of the aggregates, the species formed after overnight incubation showed a clear increase in the ThT fluorescence signal, when compared to the pre-amyloid structure (Figure 5A). They also lost their capacity to bind ANS (Figure 5B). Furthermore, after Congo Red staining some aggregates showed green birefringence when viewed under polarized light (Figure 6). However, other aggregate types were detected which were not birefringent. This heterogeneity of the assembled species suggests the existence of competing pathways of aggregation. Mixed aggregate structures have been previously reported for other proteins in vitro and in vivo (*22*). FTIR analysis of secondary structure elements of the aggregates obtained after overnight incubation at 600 MPa (Figure 3C) was performed similarly to that of the native protein and the pre-amyloid structures. The spectrum of the overnight treated aggregates was better resolved, suggesting a narrowing of the IR-bands. Determination of fractional band intensities (Table 1) indicates that, with respect to the pre-amyloid aggregates, the α-helix content did not change significantly. However, the β-sheet content increased further from 22 to 33%, and the content of unordered structures decreased from 31 to 19%.

Overnight Incubation at 600 MPa Results in the Formation of Amyloid Fibrils. TEM revealed the formation of a dense meshwork of fibrillar structure indicating a highly packed nature of the aggregates formed after overnight incubation at 600 MPa. The fibrils formed bundles, possibly by their lateral association (Figure 4C−E). The diameter of an individual fibril can be estimated as 5−10 nm. To discern whether the conformational change obtained after overnight incubation was originated by pressure treatment or was a

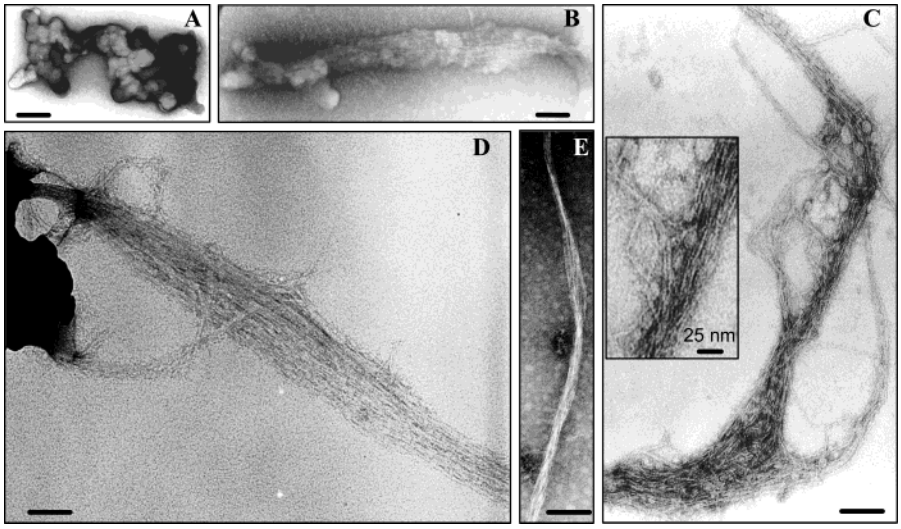

FIGURE 4: Negative-stained TEM micrographs of PrP aggregates obtained after compression at 600 MPa. (A, B) PrP aggregates generated after transient treatment at 600 MPa. (C−E) PrP aggregates obtained after overnight incubation at 600 MPa. (Bars = 100 nm).

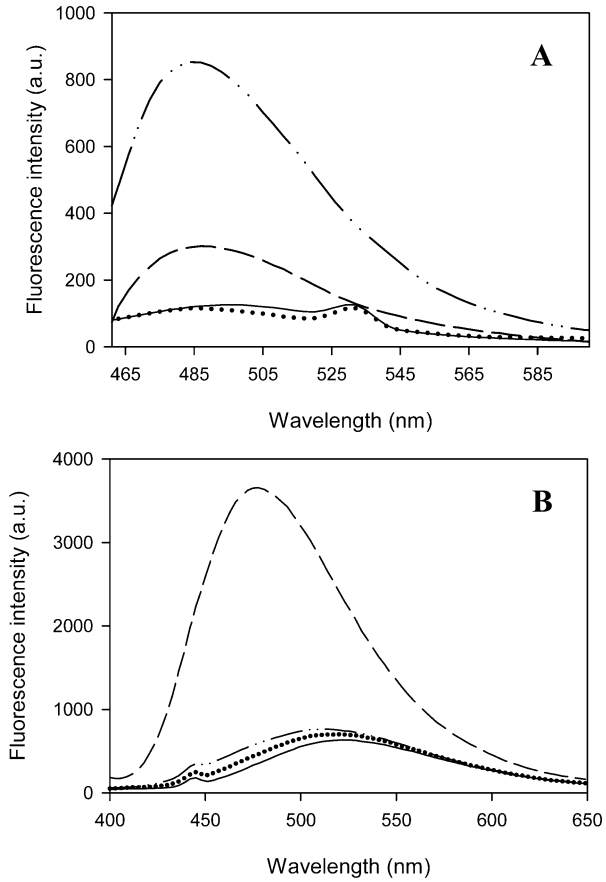

FIGURE 5: Fluorescence emission spectra of ThT (A) and ANS (B) in the absence of protein (solid line), in the presence of native PrP (dotted line), in the presence of pressure-induced aggregates generated after transient treatment at 600 MPa (dashed line), and of aggregates obtained after overnight incubation at 600 MPa (dashed and dotted line).

time-dependent process at specific temperature conditions, we incubated the pre-amyloid aggregates overnight at atmospheric pressure. However, no significant changes of the pre-amyloid structures were observed within 24 h (results not shown). In other experiments, we increased the protein concentration to 5 mg/mL. However, the pressure at which the aggregation process started was the same as in the experiments using 2 mg/mL protein concentration. In addition, FTIR and electron microscopy did not reveal any differences in secondary structure and ultrastructure between samples containing 2 and 5 mg/mL protein, which had been incubated overnight at 600 MPa (results not shown). All these characteristics indicate that the pre-amyloid structures converted into amyloid fibrils upon prolonged incubation at 600 MPa, when the protein concentration was at least 2 mg/mL.

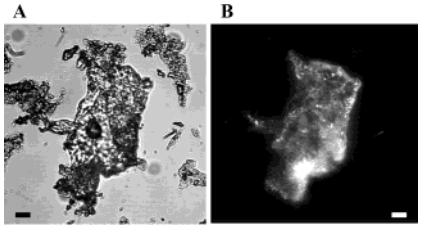

FIGURE 6: Congo red birefringence in pressure-induced PrP aggregates formed after overnight incubation at 600 MPa. Aggregates were stained with Congo red and observed under bright field (A) or by polarization microscopy (B). (Bars = 10 μm).

Resistance to Limited Proteolysis. Both aggregates—pre-amyloid structures and amyloid fibrils—were resistant to digestion by PK, even when incubated with PK at a ratio of PrP:PK = 3:1 for 1 h at 37 °C (Figure 7). However, the monomeric and soluble protein showed no apparent PK-resistant core. It was completely digested upon incubation with PK.

DISCUSSION

In Vitro versus In Vivo Process. High-pressure treatment triggers formation of two β-sheet-rich and protease-resistant insoluble prion protein structures. The first one appears to be a precursor of amyloid structures, and the second one, obtained after prolonged incubation at high pressure, adopts the form of amyloid fibrils and shares certain features with the infectious isoform. These findings are important both from a theoretical point of view and for practical applications. Indeed, they inform us about the possible structural characteristics of the pathogenic species and on the mechanism through which it may be formed. However, it should be kept in mind that conformational changes of prion protein in vivo occur in a cellular environment and may necessitate the interaction with other molecular partners such as molecular

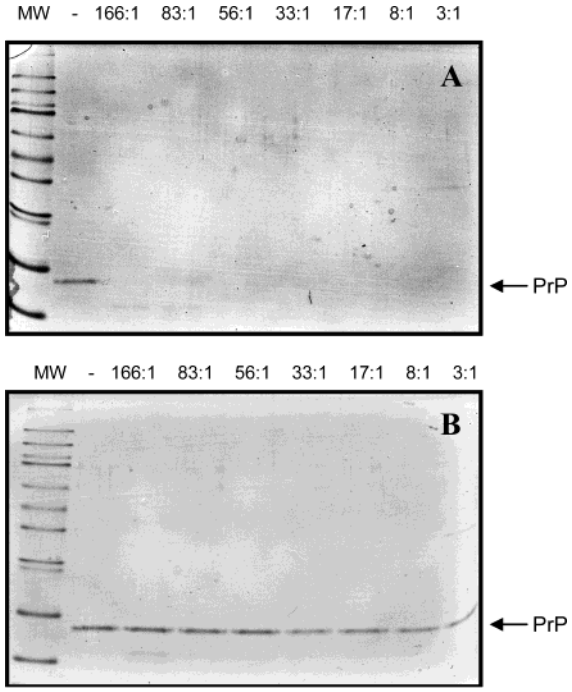

FIGURE 7: PK analysis, on 17.5% SDS−PAGE gels, of soluble PrP (A) and pressure-induced aggregates (B). Lane 1: MW, molecular mass standards; lane 2: protein in the absence of PK; lanes 3−9: protein treated with increasing concentrations of PK (the PrP/PK ratio is indicated above each lane).

chaperones, DNA, RNA, or sulfated glycans (*23*−*29*). Therefore, the similarity of the pressure-induced structural changes with the in vivo mechanism is intriguing, as pressure may substitute for some of the specific molecular interactions required in the in vivo transconformation.

Structural Changes and Aggregation under High Pressure. Our previous study (*11*), which was restricted to a low protein concentration (0.5−0.8 mg/mL), revealed alternative pathways in PrP folding and unfolding under high-pressure conditions. Independently, Kuwata et al. came to similar conclusions in a high-pressure NMR study (*30*). In addition, a very recent study reported the stabilization of folding intermediates of recombinant murine PrP using a combination of pressure and low-temperature analyses (*31*). However, no pressure-induced protein aggregation was detected. Instead, we observed in the low protein concentration range and at pressures greater than 450 MPa a metastable structure capable of binding ThT, probably a soluble oligomer (*11*). In the present study, where we have worked at a higher protein concentration (typically 2 mg/mL), the above-mentioned intermediate underwent further conformational changes and aggregated irreversibly. These conformational changes were characterized by intrinsic Trp and Tyr fluorescence and by the use of two extrinsic fluorescent probes, ANS and ThT.

The pressure-induced red-shift of Trp fluorescence indicates that hydrophobic parts of the protein became water exposed. The protein part undergoing this structural change is probably the region expanding residues 90−167, which encompasses helix 1, the β-strands, and the flexible unstructured N-terminal part of the molecule. This region is located in the outer shell of the well-structured domain made up of helix 1 and 2, and contains the two Trp residues of $SHaPrP_{90-231}$. Specifically, Trp99 is positioned at the disordered N-terminal part (residues 90−124) and Trp145 at the beginning of helix 1. The disappearance of the Tyr contribution to the emission spectrum suggests a Tyr−Trp energy transfer, which may be explained by increased intermolecular interactions in the course of the aggregation process. Interestingly, the fluorescence intensity of ANS and ThT increased simultaneously with the aggregation of the protein. ANS binds specifically to large hydrophobic protein regions which are solvent exposed (*32*). These are typically encountered in partially unfolded proteins, such as molten globule states. ThT has been shown to bind to amyloid structures and to oligomeric proteins (*33*, *34*). Therefore, these fluorescence results indicate that high pressure is not completely unfolding PrP, but instead induce a misfolded conformation containing water-exposed well-structured hydrophobic domains. At a sufficiently high protein concentration ($\geq$2 mg/mL) intermolecular collapse of these domains eventually provokes protein aggregation.

Formation of Preamyloid Structures. When the PrP aggregate, obtained after transient treatment at 600 MPa and pressure release, was suspended in buffer, its fluorescence characteristics (intrinsic fluorescence, as well as ANS and ThT fluorescence) were very similar to those of the protein recorded under high pressure. Given the irreversibility of the fluorescence spectral changes, this indicates that the structure of the aggregate was similar at atmospheric and high pressure. Nevertheless, we would like to stress that its secondary structure was determined only at atmospheric pressure, and a definitive structural comparison of the aggregates at ambient and high pressure awaits further FTIR studies using a diamond anvil cell. ThT fluorescence, as well as electron microscopy, suggest that the aggregates formed after transient high pressure treatment and decompression can be classified as pre-amyloid structures. Interestingly, their secondary structure reveals a strongly increased β-sheet content with respect to the native form, and an increased resistance to proteolysis, similarly to what is expected for the infectious PrP^{Sc} form. It is therefore possible that the pre-amyloid form is on the pathogenic pathway, or is itself infectious.

Formation of Amyloid Fibrils. Electron microscopy clearly reveals the formation of fibrils and bundles of fibrils after prolonged incubation of the pre-amyloid structures at high pressure. The strongly increased ThT fluorescence, together with the birefringence of polarized light after Congo Red staining, identifies these aggregates as amyloid fibrils. Interestingly, their secondary structure differs from that of the pre-amyloid structures, with a further increase of the β-sheet content, and a relative decrease of unordered structures.

Possible Mechanism of Amyloid Fibrils Formation. Analysis of prion protein assembly into amyloid fibrils under high pressure provides general information that may be relevant also for other proteins, in particular, those implicated in amyloid-related diseases. The data presented here suggest that protein aggregation following larger conformational changes is an essential feature of amyloidogenesis under pressure. Pressure decreases the stability of the native state relative to that of the partially unfolded ensemble. A number of unfolded regions of strong β-sheet propensity (*35*, *36*) could then form intermolecular β-sheet structures eventually leading to protein oligomerization. Studies with synthetic

peptides indicate that the 125−167 hairpin subdomain possesses a high β-sheet propensity (*36*). Moreover, in $SHaPrP_{90-231}$, this region appears to be solvent accessible, as hydrogens can be easily exchanged by deuterium atoms (*20*). Conceivably, this region may act as a nucleus in the pressure-induced formation of β-sheet structure. These exposed β-sheet rich domains would then coalesce to pre-amyloid structures and further convert into amyloid fibrils.

Several lessons can be learnt from the above observations: (i) protein misfolding, occurring already in the lower pressure range, is a prerequisite to aggregate formation; (ii) a protein concentration of at least 2 mg/mL is needed for formation of aggregates at high pressure. A similar concentration dependence has been recently reported for GdnHCl-induced PrP aggregation (*37*); (iii) the formation of amyloid fibrils is preceded by pre-amyloid structures containing structured hydrophobic domains susceptible to bind ANS. The fibrillar and not infectious PrP forms obtained in previous studies by traditional unfolding/refolding approaches (using chemical denaturants) (*21*, *38*) bind ANS. In contrast, amyloid fibrils induced under pressure do not bind ANS. The incapacity of these fibrils to bind ANS may be explained by an occlusion of the ANS binding sites (exposed hydrophobic regions) due to intermolecular contacts within the fibrillar network. Thus, different perturbation approaches lead to different misfolding pathways, suggesting that a single polypeptide can misfold into multiple topologies, a process that is thought to underlie prion strain variation (*39*) and which could contribute to the difficulty of producing in vitro the pathologically misfolded conformation from recombinant PrP.

However, is still controversial whether mature amyloid fibrils, amorphous aggregates, or soluble oligomeric intermediates are the species responsible for toxicity and disease. There is evidence in some cases that pre-fibrillar aggregates are more toxic than mature fibrils (*40*, *41*). The question of whether the pressure-induced conformers obtained in this work are capable of causing neuronal degeneration and disease is still open.

The Pressure-Specific Effects. This study highlights the use of pressure to induce protein structural changes, as an alternative to heat or chemical treatments. Indeed, proteins do not follow the same unfolding pathway when submitted to different structure perturbants (*42*), leading to different unfolded states which, in some cases, have the tendency to aggregate. Because of the specific structural effects of pressure, several high-pressure studies of proteins implicated in protein conformational diseases have been carried out, providing new insights into the fundamentals of the aggregation phenomenon (*10*, *43*, *44*). In another study, the unfolding behavior of yeast prion URE2 under pressure, facilitated by combination with nondenaturing concentrations of GdnHCl, was examined (*45*). This approach is proving particularly fruitful to extend the application of the pressure unfolding method to a wider range of systems (*46*).

How can we explain the pressure-specific effects? High pressure alters the conformation of a protein, leading to a state that occupies a smaller volume and that frequently exhibits the characteristics of a molten globule-like structure (*9*, *47*). The volume change (ΔV_U) of the pressure-induced conformational transition arises from contributions of protein internal cavities and of interactions with water (*48*, *49*). The observed ΔV_U change on pressure unfolding for $SHaPrP_{90-231}$ is approximately −30 mL/mol at pH 7 and 40 °C (*11*). As discussed by Hummer et al. (*50*), pressure-induced unfolding is caused by the penetration of water into the protein hydrophobic core. This process is due to dissociation of electrostatic bonds and to solvation of hydrophobic residues. Because of such particular properties, pressure allows subunit dissociation of oligomeric proteins, and it may avoid aggregation of protein folding intermediates and rescue native protein from aggregates. These phenomena are observed with several protein models (*10*, *46*), recently with the heat-induced amorphous aggregates of $SHaPrP_{90-231}$ (*11*), and also with amyloid fibrils of α-synuclein and transthyretin (*43*). The dissociation of such aggregates occurs in the same pressure range of that required for the dissociation of oligomeric proteins (<300 MPa) (*9*, *10*, *46*). All these findings suggest that packing defects and hydrophobic pockets are present in such different aggregated structures, and account for their pressure sensitivity. In contrast, our results with PrP indicate the formation of well-packed amyloid fibrils, exhibiting no structured hydrophobic domains at the protein surface where compounds such as ANS can bind. These fibrillar structures are insensitive to pressure dissociation, indicating a much tighter packing than in the case of α-synuclein and transthyretin, or in the case of heat-induced PrP aggregates. Hence, different pathways of aggregation and amyloid formation can lead to a different degree of compactness of final structures.

Amyloid propagation is normally highly sequence specific. In PrP, this specificity leads to the "species barrier" phenomenon, which obstructs or slows down transmission (*51*−*54*). Accordingly, a specific pattern of molecular interactions, rather than nonspecific interactions, should play a role in the formation of amyloid structures. The attractive nonbonded interactions between aromatic rings (π-stacking) show negative volume changes and are favored under pressure (*55*). In addition, studies of model systems show that hydrogen bonds are stabilized by high pressure (*55*). Therefore, it is conceivable that stacking interactions and/or stabilized hydrogen bonds between newly formed β-sheet strands may contribute energetically as well as directionally in the assembly of well-packed amyloid structures. Because high-pressure reduces cavities, we can speculate that the smaller interatomic distances between some hydrogen-bonded atoms become structural determinants when water from the protein hydration shell is excluded or better packed at high pressure. Thus, overnight incubation at high pressure may stabilize new hydrogen bonds by preventing solvation of unpaired amides and carbonyls. This idea is supported by a recent study using molecular dynamics simulations which demonstrates the role of side-chain hydrogen bonds and of aromatic stacking in the stabilization of amyloid structures (*56*).

Conclusion. The in vitro transformation of recombinant PrP into a scrapie-like aggregate which is PK resistant and shows amyloid characteristics may pave the way for structure-based drug design studies pointed to interfere with aggregation or to prevent amyloid-related toxicity. These drugs could be selected for their capacity to bind to the aggregates or for their stabilizing power of intermediate conformers, thus preventing their conversion to amyloid fibrils. It would be interesting now to further characterize structurally the

pressure-induced fibrils by methods such as atomic force microscopy or NMR for their eventual use as topological templates to generate tools for diagnostics and therapy (TSE-specific antibodies for misfolded PrP) in vitro and possibly ultimately in vivo.

ACKNOWLEDGMENT

J.T. acknowledges an INSERM postdoctoral fellowship. The plasmid containing the gene encoding PrP was a generous gift from S. B. Prusiner. We are grateful to K. Heremans and C. Dirix for secondary structure predictions. We also thank May C. Morris for corrections and critical reading of the manuscript.

REFERENCES

1. Prusiner, S. B. (1997) Prion diseases and the BSE crisis, *Science 278*, 245−251.
2. Carrell, R. W., and Lomas, D. A. (1997) Conformational disease, *Lancet 350*, 134−138.
3. Prusiner, S. B., Scott, M. R., DeArmond, S. J., and Cohen, F. E. (1998) Prion protein biology, *Cell 93*, 337−348.
4. Oesch, B., Westaway, D., Walchli, M., McKinley, M. P., Kent, S. B., Aebersold, R., Barry, R. A., Tempst, P., Teplow, D. B., Hood, L. E., et al. (1985) A cellular gene encodes scrapie PrP 27−30 protein, *Cell 40*, 735−746.
5. Stahl, N., Borchelt, D. R., Hsiao, K., and Prusiner, S. B. (1987) Scrapie prion protein contains a phosphatidylinositol glycolipid, *Cell 51*, 229−240.
6. Cohen, F. E., and Prusiner, S. B. (1998) Pathologic conformations of prion proteins, *Annu. Rev. Biochem. 67*, 793−819.
7. Glockshuber, R. (2001) Folding dynamics and energetics of recombinant prion proteins, *Adv. Protein Chem. 57*, 83−105.
8. Jonas, J. (2002) High-resolution nuclear magnetic resonance studies of proteins, *Biochim. Biophys. Acta 1595*, 145−159.
9. Silva, J. L., Foguel, D., and Royer, C. A. (2001) Pressure provides new insights into protein folding, dynamics and structure, *Trends Biochem. Sci. 26*, 612−618.
10. Randolph, T. W., Seefeldt, M., and Carpenter, J. F. (2002) High hydrostatic pressure as a tool to study protein aggregation and amyloidosis, *Biochim. Biophys. Acta 1595*, 224−234.
11. Torrent, J., Alvarez-Martinez, M. T., Heitz, F., Liautard, J. P., Balny, C., and Lange, R. (2003) Alternative prion structural changes revealed by high pressure, *Biochemistry 42*, 1318−1325.
12. Alvarez-Martinez, M. T., Torrent, J., Lange, R., Verdier, J. M., Balny, C., and Liautard, J. P. (2003) Optimized overproduction, purification, characterization and high-pressure sensitivity of the prion protein in the native (PrP(C)-like) or amyloid (PrP(Sc)-like) conformation, *Biochim. Biophys. Acta 1645*, 228−240.
13. Kitamura, Y., and Itoh, T. (1987) Reaction volume of protonic ionization for buffering agents − Prediction of pressure-dependence of pH and pOH, *J. Solution Chem. 16*, 715−725.
14. Mehlhorn, I., Groth, D., Stockel, J., Moffat, B., Reilly, D., Yansura, D., Willett, W. S., Baldwin, M., Fletterick, R., Cohen, F. E., Vandlen, R., Henner, D., and Prusiner, S. B. (1996) High-level expression and characterization of a purified 142-residue polypeptide of the prion protein, *Biochemistry 35*, 5528−5537.
15. Zhang, H., Stockel, J., Mehlhorn, I., Groth, D., Baldwin, M. A., Prusiner, S. B., James, T. L., and Cohen, F. E. (1997) Physical studies of conformational plasticity in a recombinant prion protein, *Biochemistry 36*, 3543−3553.
16. Byler, D. M., and Susi, H. (1986) Examination of the secondary structure of proteins by deconvolved FTIR spectra, *Biopolymers 25*, 469−487.
17. Goormaghtigh, E., Cabiaux, V., and Ruysschaert, J. M. (1990) Secondary structure and dosage of soluble and membrane proteins by attenuated total reflection Fourier transform infrared spectroscopy on hydrated films, *Eur. J. Biochem. 193*, 409−420.
18. Smeller, L., Goossens, K., and Heremans, K. (1995) How to minimize certain artifacts in Fourier self-deconvolution, *Appl. Spectrosc. 10*, 1538−1542.
19. James, T. L., Liu, H., Ulyanov, N. B., Farr-Jones, S., Zhang, H., Donne, D. G., Kaneko, K., Groth, D., Mehlhorn, I., Prusiner, S. B., and Cohen, F. E. (1997) Solution structure of a 142-residue recombinant prion protein corresponding to the infectious fragment of the scrapie isoform, *Proc. Natl. Acad. Sci. U.S.A. 94*, 10086−10091.
20. Liu, H., Farr-Jones, S., Ulyanov, N. B., Llinas, M., Marqusee, S., Groth, D., Cohen, F. E., Prusiner, S. B., and James, T. L. (1999) Solution structure of Syrian hamster prion protein rPrP(90−231), *Biochemistry 38*, 5362−5377.
21. Baskakov, I. V., Legname, G., Baldwin, M. A., Prusiner, S. B., and Cohen, F. E. (2002) Pathway complexity of prion protein assembly into amyloid, *J. Biol. Chem. 277*, 21140−21148.
22. Kim, Y. S., Randolph, T. W., Stevens, F. J., and Carpenter, J. F. (2002) Kinetics and energetics of assembly, nucleation, and growth of aggregates and fibrils for an amyloidogenic protein. Insights into transition states from pressure, temperature, and co-solute studies, *J. Biol. Chem. 277*, 27240−27246.
23. Stockel, J., and Hartl, F. U. (2001) Chaperonin-mediated de novo generation of prion protein aggregates, *J. Mol. Biol. 313*, 861−872.
24. Cordeiro, Y., Machado, F., Juliano, L., Juliano, M. A., Brentani, R. R., Foguel, D., and Silva, J. L. (2001) DNA converts cellular prion protein into the beta-sheet conformation and inhibits prion peptide aggregation, *J. Biol. Chem. 276*, 49400−49409.
25. Zou, W. Q., Zheng, J., Gray, D. M., Gambetti, P., and Chen, S. G. (2004) Antibody to DNA detects scrapie but not normal prion protein, *Proc. Natl. Acad. Sci. U.S.A. 101*, 1380−1385.
26. Caughey, B., and Kocisko, D. A. (2003) Prion diseases: a nucleic-acid accomplice? *Nature 425*, 673−674.
27. Deleault, N. R., Lucassen, R. W., and Supattapone, S. (2003) RNA molecules stimulate prion protein conversion, *Nature 425*, 717−720.
28. Weiss, S., Proske, D., Neumann, M., Groschup, M. H., Kretzschmar, H. A., Famulok, M., and Winnacker, E. L. (1997) RNA aptamers specifically interact with the prion protein PrP, *J. Virol. 71*, 8790−8797.
29. Warner, R. G., Hundt, C., Weiss, S., and Turnbull, J. E. (2002) Identification of the heparan sulfate binding sites in the cellular prion protein, *J. Biol. Chem. 277*, 18421−18430.
30. Kuwata, K., Li, H., Yamada, H., Legname, G., Prusiner, S. B., Akasaka, K., and James, T. L. (2002) Locally disordered conformer of the hamster prion protein: a crucial intermediate to PrPSc? *Biochemistry 41*, 12277−12283.
31. Martins, S. M., Chapeaurouge, A., and Ferreira, S. T. (2003) Folding intermediates of the prion protein stabilized by hydrostatic pressure and low temperature, *J. Biol. Chem. 278*, 50449−50455.
32. Engelhard, M., and Evans, P. A. (1995) Kinetics of interaction of partially folded proteins with a hydrophobic dye: evidence that molten globule character is maximal in early folding intermediates, *Protein Sci. 4*, 1553−1562.
33. LeVine, H., 3rd. (1993) Thioflavine T interaction with synthetic Alzheimer's disease beta-amyloid peptides: detection of amyloid aggregation in solution, *Protein Sci. 2*, 404−410.
34. Carrotta, R., Bauer, R., Waninge, R., and Rischel, C. (2001) Conformational characterization of oligomeric intermediates and aggregates in beta-lactoglobulin heat aggregation, *Protein Sci. 10*, 1312−1318.
35. Dima, R. I., and Thirumalai, D. (2002) Exploring the propensities of helices in PrP(C) to form beta sheet using NMR structures and sequence alignments, *Biophys. J. 83*, 1268−1280.
36. Jamin, N., Coic, Y. M., Landon, C., Ovtracht, L., Baleux, F., Neumann, J. M., and Sanson, A. (2002) Most of the structural elements of the globular domain of murine prion protein form fibrils with predominant beta-sheet structure, *FEBS Lett. 529*, 256−260.
37. Sokolowski, F., Modler, A. J., Masuch, R., Zirwer, D., Baier, M., Lutsch, G., Moss, D. A., Gast, K., and Naumann, D. (2003) Formation of critical oligomers is a key event during conformational transition of recombinant syrian hamster prion protein, *J. Biol. Chem. 278*, 40481−40492.
38. Baskakov, I. V., Legname, G., Prusiner, S. B., and Cohen, F. E. (2001) Folding of prion protein to its native alpha-helical conformation is under kinetic control, *J. Biol. Chem. 276*, 19687−19690.
39. Collinge, J. (2001) Prion diseases of humans and animals: their causes and molecular basis, *Annu. Rev. Neurosci. 24*, 519−550.
40. Lashuel, H. A., Hartley, D., Petre, B. M., Walz, T., and Lansbury, P. T., Jr. (2002) Neurodegenerative disease: amyloid pores from pathogenic mutations, *Nature 418*, 291.
41. Kayed, R., Head, E., Thompson, J. L., McIntire, T. M., Milton, S. C., Cotman, C. W., and Glabe, C. G. (2003) Common structure

of soluble amyloid oligomers implies common mechanism of pathogenesis, *Science 300*, 486-489.
42. Balny, C., Masson, P., and Heremans, K. (2002) High-pressure effects on biological macromolecules: from structural changes to alteration of cellular processes, *Biochim. Biophys. Acta. 1595*, 3−10.
43. Foguel, D., Suarez, M. C., Ferrao-Gonzales, A. D., Porto, T. C., Palmieri, L., Einsiedler, C. M., Andrade, L. R., Lashuel, H. A., Lansbury, P. T., Kelly, J. W., and Silva, J. L. (2003) Dissociation of amyloid fibrils of {alpha}-synuclein and transthyretin by pressure reveals their reversible nature and the formation of water-excluded cavities, *Proc. Natl. Acad. Sci. U.S.A. 100*, 9831−9836.
44. Ferrao-Gonzales, A. D., Palmieri, L., Valory, M., Silva, J. L., Lashuel, H., Kelly, J. W., and Foguel, D. (2003) Hydration and packing are crucial to amyloidogenesis as revealed by pressure studies on transthyretin variants that either protect or worsen amyloid disease, *J. Mol. Biol. 328*, 963−974.
45. Zhou, J. M., Zhu, L., Balny, C., and Perrett, S. (2001) Pressure denaturation of the yeast prion protein Ure2, *Biochem. Biophys. Res. Commun. 287*, 147−152.
46. Perrett, S., and Zhou, J. M. (2002) Expanding the pressure technique: insights into protein folding from combined use of pressure and chemical denaturants, *Biochim. Biophys. Acta 1595*, 210−223.
47. Mozhaev, V. V., Heremans, K., Frank, J., Masson, P., and Balny, C. (1996) High-pressure effects on protein structure and function, *Proteins 24*, 81−91.
48. Frye, K. J., and Royer, C. A. (1998) Probing the contribution of internal cavities to the volume change of protein unfolding under pressure, *Protein Sci. 7*, 2217−2222.
49. Royer, C. A. (2002) Revisiting volume changes in pressure-induced protein unfolding, *Biochim. Biophys. Acta 1595*, 201−209.
50. Hummer, G., Garde, S., Garcia, A. E., Paulaitis, M. E., and Pratt, L. R. (1998) The pressure dependence of hydrophobic interactions is consistent with the observed pressure denaturation of proteins, *Proc. Natl. Acad. Sci. U.S.A. 95*, 1552−1555.
51. Gabizon, R., and Taraboulos, A. (1997) Of mice and (mad) cows—transgenic mice help to understand prions, *Trends Genet. 13*, 264−269.
52. Raymond, G. J., Hope, J., Kocisko, D. A., Priola, S. A., Raymond, L. D., Bossers, A., Ironside, J., Will, R. G., Chen, S. G., Petersen, R. B., Gambetti, P., Rubenstein, R., Smits, M. A., Lansbury, P. T., Jr., and Caughey, B. (1997) Molecular assessment of the potential transmissibilities of BSE and scrapie to humans, *Nature 388*, 285−288.
53. Scott, M., Groth, D., Foster, D., Torchia, M., Yang, S. L., DeArmond, S. J., and Prusiner, S. B. (1993) Propagation of prions with artificial properties in transgenic mice expressing chimeric PrP genes, *Cell 73*, 979−988.
54. Telling, G. C., Scott, M., Mastrianni, J., Gabizon, R., Torchia, M., Cohen, F. E., DeArmond, S. J., and Prusiner, S. B. (1995) Prion propagation in mice expressing human and chimeric PrP transgenes implicates the interaction of cellular PrP with another protein, *Cell 83*, 79−90.
55. Van Eldik, R., Asano, T., and Le Noble, W. J. (1989) Activation and reaction volume in solution 2, *Chem. Rev. 89*, 549−688.
56. Gsponer, J., Haberthur, U., and Caflisch, A. (2003) The role of side-chain interactions in the early steps of aggregation: Molecular dynamics simulations of an amyloid-forming peptide from the yeast prion Sup35, *Proc. Natl. Acad. Sci. U.S.A. 100*, 5154−5159.

BI049939D